

Synthesis of Unstable Carbides Ag_2C_{2n} ($n = 3, 4$) and Characterization via Crystallographic Analysis of Their Double Salts with Silver(I) Trifluoroacetate

Sam C. K. Hau and Thomas C. W. Mak*

Department of Chemistry and Center of Novel Functional Molecules, The Chinese University of Hong Kong, Shatin, New Territories, Hong Kong SAR, People's Republic of China

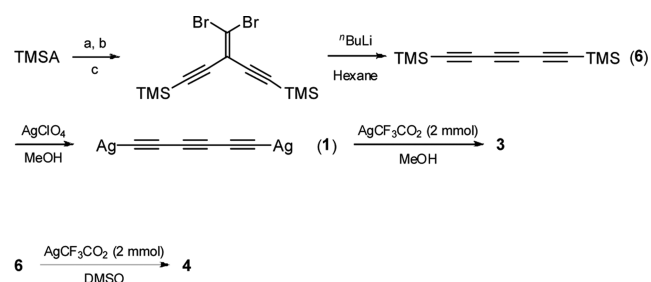
S Supporting Information

ABSTRACT: Two new silver(I) carbides, Ag_2C_6 and Ag_2C_8 , have been synthesized, and single-crystal X-ray analysis of their crystalline silver(I) trifluoroacetate complexes, $\text{Ag}_2\text{C}_6 \cdot 8\text{AgCF}_3\text{CO}_2 \cdot 6\text{H}_2\text{O}$, $4(\text{Ag}_2\text{C}_6) \cdot 16\text{AgCF}_3\text{CO}_2 \cdot 14.5\text{DMSO}$, and $2.5(\text{Ag}_2\text{C}_8) \cdot 10\text{AgCF}_3\text{CO}_2 \cdot 10\text{DMSO}$, provides detailed information on the influence of ligand disposition and orientation of the all-carbon anionic ligands in the construction of multidimensional supramolecular structures, which are consolidated by argentophilic and weak inter-/intramolecular interactions.

Over the past decade, transition metal complexes containing the linear $\text{M}-\text{C}\equiv\text{C}-(\text{C}\equiv\text{C})_n-\text{C}\equiv\text{C}-\text{M}$ ($n = 1, 2$) moiety, in which each terminal metal center ($\text{M} = \text{Re},^{1a} \text{Au},^{1b} \text{Fe},^{1c} \text{Ru},^2 \text{Os},^3 \text{Pt},^4$) is also coordinated by other ligands, have aroused much interest in view of their potential application as intriguing structure building blocks owing to their unique linear structural property.^{1–4} Meanwhile, our group has conducted a systematic investigation on the synthesis and structural characterization of a series of Ag(I) multiple salts containing silver carbide, Ag_2C_{2n} ($n = 1, 2$), as a component, in which the all-carbon dianion ethynediide, C_2^{2-} , is generally capsulated inside a polyhedral Ag_m ($m = 6–10$) cage, whereas 1,3-butadiyne-1,4-diide, C_4^{2-} , exhibits variable coordination modes involving each terminal triple bond and a Ag_m ($m = 3–5$) basket.^{5,6} Herein we report the first successful synthesis of their unstable higher homologues, silver(I) 1,3,5-hexatriyne-1,6-diide (Ag_2C_6 , **1**) and silver(I) 1,3,5,7-octatetrayne-1,8-diide (Ag_2C_8 , **2**), together with the crystal structures of three polymeric Ag(I) double salts, $\text{Ag}_2\text{C}_6 \cdot 8\text{AgCF}_3\text{CO}_2 \cdot 6\text{H}_2\text{O}$ (**3**),⁷ $4(\text{Ag}_2\text{C}_6) \cdot 16\text{AgCF}_3\text{CO}_2 \cdot 14.5\text{DMSO}$ (**4**),⁸ and $2.5(\text{Ag}_2\text{C}_8) \cdot 10\text{AgCF}_3\text{CO}_2 \cdot 10\text{DMSO}$ (**5**).⁹

Preparation of $\text{TMS}-\text{C}\equiv\text{C}-\text{C}\equiv\text{C}-\text{C}\equiv\text{C}-\text{TMS}$ (**6**) according to literature procedures^{10–12} involved two key reactions, Corey–Fuchs olefination¹³ and carbene rearrangement reaction.^{12,14} Reaction of **6** with AgClO_4 in a 1:2 molar ratio in MeOH at 23 °C for 30 min produced an orange precipitate containing Ag_2C_6 (**1**), which was filtered out and washed with deionized water (Scheme 1). [**Caution!** This crude orange Ag_2C_6 amorphous powder, being insoluble in polar or nonpolar solvents, is more explosive in the dry state than its lower homologues Ag_2C_2 and Ag_2C_4 and could only be stored in the wet form for 1–2 days in a refrigerator at -10 °C. In addition, **1** gradually darkened in color, which indicated slow decom-

Scheme 1. Synthesis of Silver(I) Double Salts **3** and **4**^a



^aReagents and conditions: (a) ⁿBuLi, (EtO)CHO, Et₂O, 0 °C; (b) PCC, CH₂Cl₂; (c) CBr₄, PPh₃, CH₂Cl₂.

position during storage. Attempts to measure its IR or Raman spectra were unsuccessful due to its instability to heat and mechanical shock.]

Orange block-like crystals of the double salt $\text{Ag}_2\text{C}_6 \cdot 8\text{AgCF}_3\text{CO}_2 \cdot 6\text{H}_2\text{O}$ (**3**)⁷ were obtained from the crystallization of crude **1** in a concentrated aqueous solution of AgCF_3CO_2 (Scheme 1). In the crystal structure of **3**, the C_6^{2-} ion is located at an inversion center, each terminal C atom being capsulated by a butterfly-shaped Ag_4 basket via the $\mu_4-\eta^1, \eta^1, \eta^1, \eta^1$ mode (Figure 1a). Exterior silver atom Ag5 is attached to the Ag_4 aggregate through a pair of $\mu_3-\eta^1, \eta^2$ trifluoroacetate groups (abbreviated as O1·O2 and O7·O8). The resulting barbell-like [$\text{Ag}_5\text{C}_6\text{Ag}_5$] aggregate exhibits quasi- C_{2h} symmetry with a plane passing through atoms Ag3, Ag4, Ag5, Ag3A, Ag4A, and Ag5A (Figure 1b). The Ag···Ag distances within the Ag_4 aggregate lie in the range 2.833(14)–2.962(13) Å, suggesting the existence of significant argentophilic interactions.^{15,16} Three independent aqua ligands are attached to the Ag atoms via different coordination modes (O1W coordinates to Ag3 and Ag4 via μ_2 mode, while both O2W and O3W attach to Ag5 via μ_1 mode).

As illustrated in Figure 2a, adjacent barbell units are interconnected by two pairs of symmetry-related trifluoroacetate groups (O3·O4 and O3A·O4A; O5·O6 and O5B·O6B) to produce an infinite silver–organic layer structure, which is further stabilized by additional H-bonding between trifluoroacetate groups and aqua ligand O1W (O1W···O4A, 2.825(12) Å; O1W···O6A, 2.836(12) Å).

Received: November 27, 2013

Published: January 3, 2014

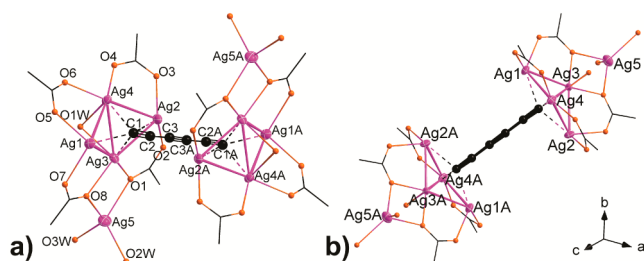


Figure 1. (a) Coordination environment of the Ag(I) atoms in double salt $\text{Ag}_2\text{C}_6 \cdot 8\text{AgCF}_3\text{CO}_2 \cdot 6\text{H}_2\text{O}$ (**3**). The argentophilic Ag...Ag distances shown as thick rods lie in the range 2.70–3.40 Å, and the H and F atoms are omitted for clarity. Silver atoms are drawn as thermal ellipsoids (50% probability level) with atom labeling. (b) Perspective view of the barbell-like $[\text{Ag}_5\text{C}_6\text{Ag}_5]$ aggregate with a pseudo-mirror plane passing through atoms Ag3, Ag4, and Ag5 and their symmetry equivalents. Color scheme: purple, Ag; orange, O; broken lines, Ag–C bonds; the same color scheme for atoms and bonds applies to all other figures.

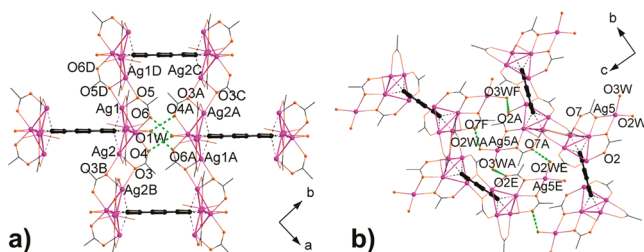


Figure 2. Perspective view of the crystal packing in **3** along (a) the *c*-axis and (b) the *a*-axis, showing notable H-bonds. Green broken lines indicate H-bond interactions; henceforth the same representation will apply to other crystal packing figures.

Further association of neighboring silver–organic layers through additional H-bonding involving the other two aqua ligands and trifluoroacetate groups ($\text{O2A} \cdots \text{O3WB}$, 2.743(15) Å; $\text{O2WA} \cdots \text{O7B}$, 2.790(14) Å) gives a 3-D supramolecular network (Figure 2b).

Starting material **6** was first added to a concentrated DMSO^{17} solution of AgCF_3CO_2 , quickly yielding an orange Ag_2C_6 precipitate, which gradually dissolved to form a deep red clear solution (Scheme 1). Transparent, orange plates of the double salt $4(\text{Ag}_2\text{C}_6) \cdot 16\text{AgCF}_3\text{CO}_2 \cdot 14.5\text{DMSO}$ (**4**)⁸ gradually crystallized through diffusion from atmospheric moisture into this deep red solution. Complex **4** contains five crystallographically independent C_6^{2-} ions, two located at crystallographic inversion centers (Figure 3). Among the five $[\text{Ag}_4\text{C}_6\text{Ag}_3]$ and $[\text{Ag}_4\text{C}_6\text{Ag}_4]$ aggregates, the eight independent terminal ethynide moieties exhibit different coordination modes: $\mu_4\text{-}\eta^1, \eta^1, \eta^1, \eta^2$ for $\text{C1} \equiv \text{C2}$, $\text{C8} \equiv \text{C9}$, and $\text{C10} \equiv \text{C11}$; $\mu_3\text{-}\eta^1, \eta^1, \eta^1$ for $\text{C4} \equiv \text{C5}$ and $\text{C20} \equiv \text{C21}$; $\mu_4\text{-}\eta^1, \eta^1, \eta^1, \eta^1$ for $\text{C14} \equiv \text{C15}$ and $\text{C16} \equiv \text{C17}$; and $\mu_4\text{-}\eta^1, \eta^1, \eta^2, \eta^2$ for $\text{C22} \equiv \text{C23}$. Besides this, such supramolecular synthons¹⁸ coalesce with their adjacent units through argentophilic interactions, with Ag...Ag bond distances ranging 2.746(3)–3.573(2) Å, comparable to those observed in a wide variety of silver double and multiple salts,¹⁶ to yield a pair of symmetry-related infinite silver chains (Type I and II), which point in opposite directions (Figure S1). As a result, a 1-D distorted ladder-like silver double-chain structure is generated (Figure S2).

The Ag–C bond distances between the Ag caps and C_8^{2-} dianions lie in the ranges 2.12(1)–2.15(2), 2.42(2)–2.45(2),

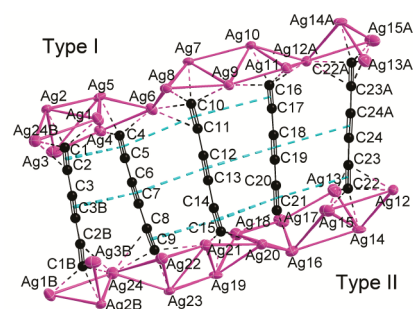


Figure 3. Coordination environment of five independent $[\text{Ag}_4\text{C}_6\text{Ag}_3]$ and $[\text{Ag}_4\text{C}_6\text{Ag}_4]$ aggregates in double salt $4(\text{Ag}_2\text{C}_6) \cdot 16\text{AgCF}_3\text{CO}_2 \cdot 14.5\text{DMSO}$ (**4**), showing notable π – π stacking interactions. The argentophilic Ag...Ag distances shown as thick rods lie in the range 2.70–3.60 Å, and the H and F atoms are omitted for clarity. Silver atoms are drawn as thermal ellipsoids (50% probability level) with atom labeling. Turquoise broken lines indicate π – π stacking interactions; henceforth the same representation will apply to other figures.

and 2.13(2)–2.86(2) Å for σ , π , and mixed (σ, π) interactions, respectively, according to the classification in our previous studies.¹⁹ The lengths of the C–C triple and single bonds are in the ranges 1.19(3)–1.30(3) and 1.34(3)–1.38(3) Å, respectively, consistent with the corresponding values in our previous observation for those complexes containing C_4^{2-} dianion.²⁰

In addition, the ladder-like silver double-chain structures are further consolidated by offset π – π interactions between proximal triple bonds of adjacent C_6^{2-} dianions [bond center–bond center distances (Å) in the range 3.60–4.00 Å: $\text{C1} \equiv \text{C2} \cdots \text{C4} \equiv \text{C5}$, 3.683(3); $\text{C1B} \equiv \text{C2B} \cdots \text{C4B} \equiv \text{C5B}$, 3.683(3); $\text{C3} \equiv \text{C3B} \cdots \text{C6} \equiv \text{C7}$, 3.826(3); $\text{C3} \equiv \text{C3B} \cdots \text{C7B} \equiv \text{C6B}$, 3.825(3); $\text{C4} \equiv \text{C5} \cdots \text{C10} \equiv \text{C11}$, 3.808(4); $\text{C6} \equiv \text{C7} \cdots \text{C12} \equiv \text{C13}$, 3.759(3); $\text{C8} \equiv \text{C9} \cdots \text{C14} \equiv \text{C15}$, 3.858(3); $\text{C10} \equiv \text{C11} \cdots \text{C16} \equiv \text{C17}$, 3.848(4); $\text{C12} \equiv \text{C13} \cdots \text{C18} \equiv \text{C19}$, 3.714(3); $\text{C14} \equiv \text{C15} \cdots \text{C20} \equiv \text{C21}$, 3.869(3); $\text{C18} \equiv \text{C19} \cdots \text{C24A} \equiv \text{C24}$, 3.650(3); $\text{C18A} \equiv \text{C19A} \cdots \text{C24} \equiv \text{C24A}$, 3.825(4); $\text{C20} \equiv \text{C21} \cdots \text{C23} \equiv \text{C22}$, 3.823(4); $\text{C20A} \equiv \text{C21A} \cdots \text{C23A} \equiv \text{C22A}$, 3.650(3)] (see Figure S4a). These distances are comparable to similar offset face-to-face π – π interactions between phenyl rings.²¹

In complex **4**, the 15 independent co-crystallized DMSO ligand molecules (O33 to O47, the last one exhibiting half site-occupancy) attached to different Ag centers take variable $\mu_1\text{-}\eta^1$, $\mu_2\text{-}\eta^1, \eta^1$, and $\mu_3\text{-}\eta^1, \eta^1, \eta^1$ coordination modes (see Figure S3). Adjacent silver–organic chains are interconnected through additional H-bonding between DMSO molecules and nearby trifluoroacetate groups ($\text{C71B} \cdots \text{H} \cdots \text{F47}$, 2.875(23) Å) to generate a Ag(I)–organic supramolecular layer (Figure 4a). Cross-linkage of such layers by weak C–H...F bonds between DMSO ligands and trifluoroacetate groups from adjacent layers [$\text{C60D} \cdots \text{H} \cdots \text{F25}$, 2.781(30) Å; $\text{C69} \cdots \text{H} \cdots \text{F15D}$, 2.605(21) Å; $\text{C68} \cdots \text{H} \cdots \text{F18D}$, 2.779(18) Å; $\text{C80E} \cdots \text{H} \cdots \text{F9}$, 2.672(42) Å] yields a 3-D supramolecular network (Figure 4b).

$\text{TMS} \text{---} \text{C} \equiv \text{C} \text{---} (\text{C} \equiv \text{C})_2 \text{---} \text{C} \equiv \text{C} \text{---} \text{TMS}$ (**7**) is synthesized according to a modified literature procedure (Scheme 2).¹² Unfortunately, crude Ag_2C_8 (**2**) cannot be isolated in powder form like **1** due to its high reactivity and explosive properties. Reaction between **7** and AgCF_3CO_2 in DMSO produced crude Ag_2C_8 as an orange precipitate, which was later dissolved to give a deep red clear solution. Orange plate-like crystals of double salt $2.5(\text{Ag}_2\text{C}_8) \cdot 10\text{AgCF}_3\text{CO}_2 \cdot 10\text{DMSO}$ (**5**) gradually

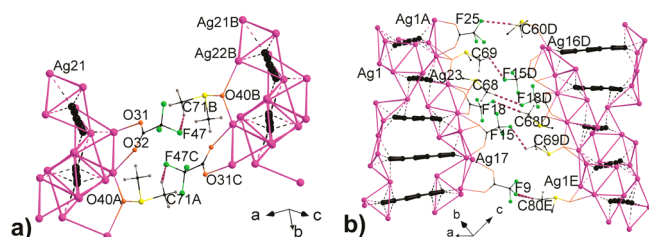
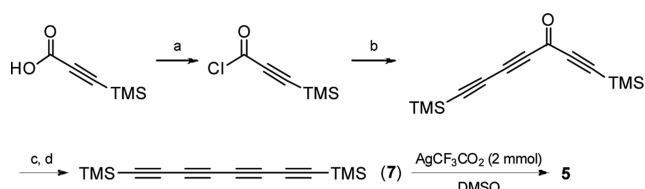


Figure 4. Perspective view of the crystal packing in **4**, along (a) the *c*-axis and (b) the *a*-axis, showing notable H-bonds. Violet broken lines indicate weak C–H...F interactions; henceforth the same representation will apply to other crystal packing figures.

Scheme 2. Synthesis of Silver(I) Double Salt **5**^a



^aReagents: (a) $(\text{COCl})_2$, DMF; (b) $(\text{TMS})_2\text{C}_4$, AlCl_3 , CH_2Cl_2 ; (c) CBr_4 , PPh_3 , CH_2Cl_2 ; (d) $^t\text{BuLi}$, C_6H_{14} .

formed through water diffusion into a concentrated $\text{AgCF}_3\text{CO}_2/\text{Ag}_2\text{C}_8$ solution in DMSO. The asymmetric unit of **5** contains three independent $[\text{Ag}_4\text{C}_8\text{Ag}_4]$ aggregates (Figure 5), one occupying a site of symmetry 1, together with 10

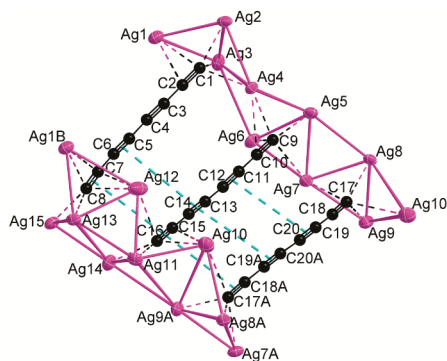


Figure 5. Coordination environment of the Ag(I) atoms in double salt $2.5(\text{Ag}_2\text{C}_8) \cdot 10\text{AgCF}_3\text{CO}_2 \cdot 10\text{DMSO}$ (**5**). The argentophilic Ag...Ag distances shown as thick rods lie in the range 2.70–3.40 Å, and the H and F atoms are omitted for clarity. Silver atoms are drawn as thermal ellipsoids (50% probability level) with atom labeling.

independent trifluoroacetate groups and 10 DMSO ligands. The Ag–C bond distances between the Ag caps and C_8^{2-} dianions are in the ranges 2.07(1)–2.11(1), 2.48(1)–2.53(1), and 2.16(1)–2.87(2) Å for σ , π , and mixed (σ, π) interactions, respectively. The lengths of the C–C triple and single bonds lie in the ranges 1.19(1)–1.24(2) and 1.33(2)–1.40(2) Å, respectively.

Such Ag_4 caps and their adjacent symmetric-related segments are fused to form a Ag_{15} aggregate through atom sharing, and such Ag_{15} aggregates are further coalesced to generate an infinite Ag chain. The three C_8^{2-} dianions further undergo offset π – π interactions [$\text{C1} \equiv \text{C2} \cdots \text{C8B} \equiv \text{C7B}$, 3.960(3) Å; $\text{C3} \equiv \text{C4} \cdots \text{C6B} \equiv \text{C5B}$, 3.891(3) Å; $\text{C5} \equiv \text{C6} \cdots \text{C4B} \equiv \text{C3B}$, 3.891(3) Å; $\text{C5} \equiv \text{C6} \cdots \text{C13} \equiv \text{C14}$, 4.058(3) Å; $\text{C7} \equiv \text{C8} \cdots \text{C2B} \equiv \text{C1B}$, 3.960(3) Å; $\text{C7} \equiv \text{C8} \cdots \text{C15} \equiv \text{C16}$, 3.782(3) Å;

$\text{C11} \equiv \text{C12} \cdots \text{C19} \equiv \text{C20}$, 3.926(3) Å; $\text{C13} \equiv \text{C14} \cdots \text{C20A} \equiv \text{C19A}$, 3.825(3) Å; $\text{C15} \equiv \text{C16} \cdots \text{C18A} \equiv \text{C17A}$, 3.772(3) Å; $\text{C17} \equiv \text{C18} \cdots \text{C16A} \equiv \text{C15A}$, 3.771(3) Å; $\text{C19} \equiv \text{C20} \cdots \text{C14A} \equiv \text{C13A}$, 3.825(3) Å; $\text{C20A} \equiv \text{C19A} \cdots \text{C12A} \equiv \text{C11A}$, 3.926(3) Å], which provide additional stability to the Ag(I) double-chain structure (Figure S4b).

The 10 independent DMSO ligands chelated on the Ag chain can be classified into three groups according to their corresponding coordination modes: $\mu_1\text{-}\eta^1$, O23; $\mu_2\text{-}\eta^1, \eta^1$, O21, O22, O24, O26, O27, O29, and O30; and $\mu_3\text{-}\eta^1, \eta^1, \eta^1$, O25 and O28 (Figure S5). Adjacent Ag(I)–organic chains are interconnected by additional H-bonds between DMSO ligands and trifluoroacetate groups [$\text{C53C} \cdots \text{H} \cdots \text{F17}$, 2.666(12) Å; $\text{C48} \cdots \text{H} \cdots \text{F15E}$, 2.661(13) Å; $\text{C59E} \cdots \text{H} \cdots \text{F24}$, 2.598(12) Å] to yield a supramolecular layer structure (Figure S6). Further cross-linking of such layer structures by weak C–H...F between DMSO ligands and trifluoroacetate groups [$\text{C49A} \cdots \text{H} \cdots \text{F8B}$, 2.536(16) Å; $\text{C41D} \cdots \text{H} \cdots \text{F21C}$, 2.605(12) Å; $\text{C42D} \cdots \text{H} \cdots \text{F27C}$, 2.619(12) Å] gives a 3-D supramolecular network structure (Figure S7).

The Ag–C \equiv C (σ -type interaction) and C \equiv C–C angles in **3–5** lie in the ranges 160.3(2)–171.4(2) $^\circ$ and 173.6(2)–179.4(2) $^\circ$, respectively, which show larger deviation from linearity ($<10^\circ$ in general) than those reported in other C_6/C_8 -bridged transition metal (Re^{1a} , Au^{1b} , Fe^{1c} , Ru^{2} , Os^{3} , Pt^{4}) complexes that are mostly dinuclear, indicating the effect of multinuclear Ag–ethynide interactions on the AgC_{2n}Ag ($n = 3, 4$) segments.

Among complexes **3–5**, the coordination mode of either C_6^{2-} or C_8^{2-} retains the highest ligation number²⁰ of 8, consistent with those established for C_2^{2-} and C_4^{2-} , featuring the co-existence of Ag(I)–C σ - and π -type bonding. Such high-nuclearity coordination mode is further stabilized by ionic as well as argentophilic interactions. The internal ethynyl groups in both C_6^{2-} and C_8^{2-} are found to have no interaction with the Ag(I) ions. Notably, they gain stabilization via offset π – π stacking between adjacent ethynyl groups, which is seldom observed in polymeric coordination networks. The coordination modes of the trifluoroacetate groups vary from the common $\mu_2\text{-}\eta^2$ kind to the $\mu_2\text{-}\eta^1, \eta^1$, $\mu_3\text{-}\eta^1, \eta^2$, and $\mu_4\text{-}\eta^2, \eta^2$ varieties. The trifluoroacetate ligand generally plays two important roles: either spanning an edge of the Ag_n basket to consolidate the $[\text{Ag}_n\text{C}\equiv\text{C}]^{(n-1)+}$ cationic moiety, or bridging adjacent Ag_n baskets to generate an infinite chain or layer structure. Complexes **3–5** all contain solvated water or DMSO molecules in their crystalline lattices. In these complexes, regular or weak C–H...F hydrogen bonds confer enhanced stability to a coordination chain/layer or connect the chains into a higher-dimensional supramolecular structure.

In summary, the present study provides the first examples of polymeric organosilver(I) frameworks assembled with the linear multinuclear Ag(I)–polyyne diene supramolecular synthons $\text{Ag}_m\text{C}\equiv\text{C}-(\text{C}\equiv\text{C})_m-\text{C}\equiv\text{C}\text{Ag}_n$ ($m = 1, 2$; $n = 3, 4$). Seen in a different light, the new Ag(I) carbides Ag_2C_6 and Ag_2C_8 , despite their inherent instability, are potentially useful as structure building units for the construction of new coordination networks in combination with coinage-metal ions, inorganic/organic anionic bridging anions, and ancillary ligands.

■ ASSOCIATED CONTENT

■ Supporting Information

Experimental details, additional figures, ^1H NMR spectra, and X-ray crystallographic data in CIF format. This material is available free of charge via the Internet at <http://pubs.acs.org>.

■ AUTHOR INFORMATION

Corresponding Author

tcwmak@cuhk.edu.hk

Notes

The authors declare no competing financial interest.

■ ACKNOWLEDGMENTS

This work is dedicated to the memory of Dr. Hson-Mou Chang (1923–2000). We gratefully acknowledge financial support by the Hong Kong Research Grants Council (GRF CUHK 402710) and the Wei Lun Foundation, and the award of a Postdoctoral Research Fellowship to S.C.K.H. by The Chinese University of Hong Kong.

■ REFERENCES

- (1) (a) $M = \text{Re}$: Yam, V. W.-Y.; Chong, S. H.-F.; Ko, C.-C.; Cheung, K.-K. *Organometallics* **2000**, *19*, 5092. (b) $M = \text{Au}$: Lu, W.; Xiang, H.-F.; Zhu, N.; Che, C.-M. *Organometallics* **2002**, *21*, 2343. (c) $M = \text{Fe}$: Akita, M.; Sakurai, A.; Moro-oka, Y. *Chem. Commun.* **1999**, 101.
- (2) $M = \text{Ru}$: (a) Qi, H.; Gupta, A.; Noll, B. C.; Snider, G. L.; Lu, Y.; Lent, C.; Fehlner, T. P. *J. Am. Chem. Soc.* **2005**, *127*, 15218. (b) Gao, L.-B.; Kan, J.; Fan, Y.; Zhang, L.-Y.; Liu, S.-H.; Chen, Z.-N. *Inorg. Chem.* **2007**, *46*, 5651. (c) Xu, G.-L.; Zou, G.; Ni, Y.-H.; DeRosa, M. C.; Crutchley, R. J.; Ren, T. *J. Am. Chem. Soc.* **2003**, *125*, 10057. (d) Xu, G.-L.; Wang, C.-Y.; Ni, Y.-H.; Goodson, T. G., III; Ren, T. *Organometallics* **2005**, *24*, 3247. (e) Xi, B.; Xu, G.-L.; Fanwick, P. E.; Ren, T. *Organometallics* **2009**, *28*, 2338. (f) Xi, B.; Liu, I. P.-C.; Xu, G.-L.; Choudhuri, M. M. R.; DeRosa, M. C.; Crutchley, R. J.; Ren, T. *J. Am. Chem. Soc.* **2011**, *133*, 15094.
- (3) $M = \text{Os}$: Bruce, M. I.; Kramarczuk, K. A.; Skelton, B. W.; White, A. H. *J. Organomet. Chem.* **2010**, *695*, 469.
- (4) $M = \text{Pt}$: (a) Stahl, J.; Bohling, J. C.; Bauer, E. B.; Peters, T. B.; Mohr, W.; Martín-Alvarez, J. M.; Hampel, T.; Gladysz, J. A. *Angew. Chem., Int. Ed.* **2002**, *41*, 1871. (b) Zheng, Q.; Gladysz, J. A. *J. Am. Chem. Soc.* **2005**, *127*, 10508. (c) Stahl, J.; Mohr, W.; de Quadras, L.; Peters, T. B.; Bohling, J. C.; Martín-Alvarez, J. M.; Owen, G. R.; Hampel, F.; Gladysz, J. A. *J. Am. Chem. Soc.* **2007**, *129*, 8282. (d) de Quadras, L.; Bauer, E. B.; Mohr, W.; Bohling, J. C.; Peters, T. B.; Martín-Alvarez, J. M.; Hampel, F.; Gladysz, J. A. *J. Am. Chem. Soc.* **2007**, *129*, 8296. (e) Owen, G. R.; Stahl, J.; Hampel, F.; Gladysz, J. A. *Chem.—Eur. J.* **2008**, *14*, 73. (f) Owen, G. R.; Gauthier, S.; Weibach, N.; Hampel, F.; Bhuvanesh, N.; Gladysz, J. A. *Dalton Trans.* **2010**, 39, 5260. (g) Yam, V. W.-Y.; Wong, K. M.-C.; Zhu, N. *Angew. Chem., Int. Ed.* **2003**, *42*, 1400. (h) Lu, W.; Mi, B.-X.; Chan, M. C. W.; Hui, Z.; Che, C.-M.; Zhu, N.; Lee, S.-T. *J. Am. Chem. Soc.* **2004**, *126*, 4958.
- (5) For reviews, see: (a) Mak, T. C. W.; Zhao, X.-L.; Wang, Q.-M.; Guo, G.-C. *Coord. Chem. Rev.* **2007**, *251*, 2311. (b) Mak, T. C. W.; Zhao, L. *Chem. Asian J.* **2007**, *2*, 456. (c) Mak, T. C. W.; Zhao, L.; Zhao, X.-L. Supramolecular Assembly of Silver(I) Complexes with Argentophilic and Silver...Carbon Interactions. In *The Importance of π -Interactions in Crystal Engineering—Frontiers in Crystal Engineering III*; Tiekink, E. R. T., Zukerman-Schpector, J., Eds.; Wiley: Chichester, 2012; Chap. 13, pp 323–366.
- (6) (a) Zhao, X.-L.; Mak, T. C. W. *Inorg. Chem.* **2010**, *49*, 3676. (b) Hu, T.; Zhao, L.; Mak, T. C. W. *Organometallics* **2012**, *31*, 7539. (c) Hu, T.; Mak, T. C. W. *Inorg. Chem.* **2013**, *52*, 9066. (d) Hu, T.; Mak, T. C. W. *Cryst. Growth Des.* **2013**, *13*, 4957.
- (7) Crystal data for **3**: $\text{C}_{22}\text{H}_{12}\text{Ag}_{10}\text{F}_{24}\text{O}_{22}$, $M = 2163.02$, monoclinic, space group $P2_1/c$ (No. 14), $a = 10.871(7)$ Å, $b = 10.844(7)$ Å, $c = 20.337(20)$ Å, $\beta = 97.983(10)^\circ$, $V = 2374.3(3)$ Å³, $Z = 2$, $T = 173$ K, $R_1 = 0.0761$, $wR_2 = 0.2052$ for 4290 reflections [$I > 2\sigma(I)$]. IR (KBr): 1928, 2047, 2129 cm^{-1} ($\nu_{\text{C}\equiv\text{C}}$, w).
- (8) Crystal data for **4**: $\text{C}_{170}\text{H}_{150}\text{Ag}_{48}\text{F}_{96}\text{O}_{93}\text{S}_{29}$, $M = 11612.40$, triclinic, space group $P\bar{1}$ (No. 2), $a = 15.124(18)$ Å, $b = 22.255(3)$ Å, $c = 26.642(3)$ Å, $\alpha = 102.224(2)^\circ$, $\beta = 97.582(2)^\circ$, $\gamma = 108.848(2)^\circ$, $V = 8097.3(16)$ Å³, $Z = 1$, $T = 173$ K, $R_1 = 0.1072$, $wR_2 = 0.3001$ for 29 018 reflections [$I > 2\sigma(I)$].
- (9) Crystal data for **5**: $\text{C}_{60}\text{H}_{60}\text{Ag}_{15}\text{F}_{30}\text{O}_{30}\text{S}_{10}$, $M = 3769.73$, monoclinic, space group $C2/c$ (No. 15), $a = 58.133(4)$ Å, $b = 11.814(9)$ Å, $c = 39.378(3)$ Å, $\beta = 129.787(10)^\circ$, $V = 20782(3)$ Å³, $Z = 8$, $T = 173$ K, $R_1 = 0.0803$, $wR_2 = 0.2266$ for 18 835 reflections [$I > 2\sigma(I)$].
- (10) Anthony, J.; Boldi, A. M.; Rubin, Y.; Hobi, M.; Gramlich, V.; Knobler, C. B.; Seiler, P.; Diederich, F. *Helv. Chim. Acta* **1995**, *78*, 13.
- (11) We are indebted to a reviewer for drawing our attention to an alternative route that gives **6** in gram scale. See: Rubin, Y.; Lin, S. S.; Knobler, C. B.; Anthony, J.; Boldi, A. M.; Diederich, F. *J. Am. Chem. Soc.* **1991**, *113*, 6943.
- (12) Eisler, S.; Slepokov, A. D.; Elliott, E.; Luu, T.; McDonald, R.; Hegmann, F. A.; Tykwinski, R. R. *J. Am. Chem. Soc.* **2005**, *127*, 2666.
- (13) Corey, E. J.; Fuchs, P. L. *Tetrahedron Lett.* **1972**, *13*, 3769.
- (14) Xu, G.-L.; Xi, B.; Updegraff, J. B.; Protasiewicz, J. D.; Ren, T. *Organometallics* **2006**, *25*, 5213.
- (15) (a) Pyykkö, P. *Chem. Rev.* **1988**, *88*, 563. (b) Pyykkö, P. *Chem. Rev.* **1997**, *97*, 597. (c) Pyykkö, P. *Chem. Soc. Rev.* **2008**, *37*, 1967. (d) Grimme, S.; Djukic, J.-P. *Inorg. Chem.* **2010**, *49*, 2911. (e) Muñiz, J.; Wang, C.; Pyykkö, P. *Chem.—Eur. J.* **2011**, *17*, 368.
- (16) (a) Guo, G.-C.; Zhou, G.-D.; Mak, T. C. W. *J. Am. Chem. Soc.* **1999**, *121*, 3136. (b) Guo, G.-C.; Zhou, G.-D.; Wang, Q.-G.; Mak, T. C. W. *Angew. Chem., Int. Ed.* **1998**, *37*, 630. (c) Wang, Q.-G.; Mak, T. C. W. *J. Am. Chem. Soc.* **2001**, *123*, 1501. (d) Wang, Q.-M.; Mak, T. C. W. *Angew. Chem., Int. Ed.* **2001**, *40*, 1130. (e) Wang, Q.-M.; Mak, T. C. W. *Chem. Commun.* **2001**, 37, 807.
- (17) DMSO was employed as it has been proven to be a good solvent by functioning as a co-ligand in our previous studies. See: Cheng, P.-S.; Marivel, S.; Zang, S.-Q.; Gao, G.-G.; Mak, T. C. W. *Cryst. Growth Des.* **2012**, *12*, 4519.
- (18) (a) Desiraju, G. R. *Angew. Chem., Int. Ed.* **1995**, *34*, 2311. (b) Desiraju, G. R. *Angew. Chem., Int. Ed.* **2007**, *46*, 8342.
- (19) Hau, S. C. K.; Mak, T. C. W. *Chem.—Eur. J.* **2013**, *19*, 5387.
- (20) Zhao, L.; Mak, T. C. W. *J. Am. Chem. Soc.* **2004**, *126*, 6852.
- (21) Janiak, C. *J. Chem. Soc., Dalton Trans.* **2000**, 3885.
- (22) Guo, G.-C.; Mak, T. C. W. *Chem. Commun.* **1999**, 813.